# Loop-expansion study of the single-hole spectral function in the $t$-$J$ model

Zhiping Liu
*Laboratory of Atomic and Solid State Physics, Cornell University, Ithaca, New York 14853*

Efstratios Manousakis
*Department of Physics, Center for Materials Research and Technology and Supercomputer Computations Research Institute, Florida State University, Tallahassee, Florida 32306*

(Received 5 July 1994)

We consider a single hole in the $t$-$J$ model where the Heisenberg and the hole-hopping terms are expanded in powers of the spin-deviation operators. The lowest order corresponds to the linear spin-wave approximation and leads to an effective Hamiltonian studied earlier by means of self-consistent perturbation theory. In this work we shall include all terms generating up to two-loop diagrams in the perturbative expansion of the single-hole Green's function. The hard-core constraints are partially respected and the overall effect gives a renormalization factor of 1.158 to the hopping parameter $t$. The vertex that describes the process where a spin wave is absorbed and emitted at the same time by the hole is far more important than others. We find that the numerical solutions of Dyson's equation including all two-loop diagrams lower considerably the single-hole ground-state energies over the previous one-loop results and our results on the $4\times4$ lattice are in better agreement with those obtained by exact diagonalization in the physical regime (small $J/t$). Our method can provide numerical solutions to the hole Green's function on very large lattices. We find that with the inclusion of the two-loop diagrams the spectral function retains all its features found in the one-loop calculation and the bandwidth, the quasiparticle residues, and the "string" excitations feel very small corrections.

## I. INTRODUCTION

The motion of a single hole in an antiferromagnetically aligned spin background is a long-standing problem[1] that concerns the electron states in localized magnetic insulators and has been studied considerably. A single hole is not in a simple Bloch state since when it hops it disturbs the antiferromagnetic arrangement of spins in the ground state and thus destroys the translational invariance. This problem has received significant attention especially since the discovery of the copper oxide superconductors,[2] where superconductivity arises from the doping of holes in an antiferromagnetic insulator. One of the simplest models for studying this problem is the $t$-$J$ model given as

$$\hat{H}_{t\text{-}J} = -t\sum_{\langle i,j\rangle\sigma}(\bar{c}^{\dagger}_{i,\sigma}\bar{c}_{j,\sigma}+\text{H.c.}) + J\sum_{\langle i,j\rangle}(1-\hat{n}^{h}_{i})\mathbf{S}_{i}\cdot\mathbf{S}_{j}(1-\hat{n}^{h}_{j}), \quad (1)$$

where $\bar{c}_{i,\sigma}$ is the constrained hole creation operator defined as $\bar{c}_{i,\sigma}=c_{i,\bar{\sigma}}(1-c^{\dagger}_{i,-\sigma}c_{i,-\sigma})$, while $c_{i,\sigma}$ denotes the annihilation operator for an electron with spin $\sigma$ on the lattice site $i$ and the hole number operator is denoted by $\hat{n}^{h}_{i}$. The assumptions undertaken here are that the spin part of the $t$-$J$ Hamiltonian has an antiferromagnetic long-range-ordered ground state and that the excitations are spin waves, which are supported in many aspects by neutron and Raman scattering experiments.[3] There are other approaches where the hole interactions with excitations corresponding to nonmagnetically ordered spin-liquid states are studied.[4,5]

Because of the lack of an exact solution to this model, various approximations have been explored to understand the basic physical implications of the model. The self-consistent approach proposed by Schmitt-Rink *et al.*[6] and Kane *et al.*[4] has proved valuable to study the single-hole dynamics in the so-called physical regime of $t/J$.[7–9] In our previous papers,[9] we approximated the $t$-$J$ model by an effective Hamiltonian $H^{(L)}_{t\text{-}J}$ where in the $J$ term only terms quadratic in the spin-deviation operators are retained [linear spin-wave (LSW) approximation] and the hopping term is linearized in the spin-deviation operators. In these papers we provided numerical solutions of the hole spectral function using a self-consistent approach where we studied one-loop as well as two- and three-loop diagrams. We found that the contribution of two-loop diagrams is exactly zero and the contribution of the leading three-loop diagrams is small; we also found reasonable agreement with exact results on the $4^2$ lattice even in the noncrossing (one-loop) approximation.

In this paper, we consider a single hole in the $t$-$J$ model where the Heisenberg and the hole-hopping terms are expanded in powers of the spin-deviation operators. At lowest order our approach corresponds to the linear spin-wave approximation and leads to the effective Hamiltonian $H^{(L)}_{t\text{-}J}$ studied earlier by means of self-consistent perturbation theory.[9] In real undoped materials a small

 

amount of anisotropy selects the direction of the staggered magnetization to be along some crystal axis and the presence of a single hole does not spoil the long-range order. In this work we shall include all terms generating up to two-loop diagrams in the perturbative expansion of the hole Green's function. At the two-loop level there are no contributions if one considers the $H_{t\text{-}J}^{(L)}$ model; however, there are several two-loop diagrams obtained by terms neglected when the $t$-$J$ model is linearized and approximated by $H_{t\text{-}J}^{(L)}$. The inclusion of two-loop diagrams improves the results as found by comparing our numerical solutions on the $4 \times 4$ lattice with exact results. We found that the restriction of no double occupancy on the same site by two spins renormalizes the hopping parameter $t$ at the two-loop level by 1.158 for an infinite square lattice, which is equal to that of the first-order higher nonlinear spin-wave correction to the energy spectrum of the linear spin-wave theory of the Heisenberg model.[10,11] The two-loop diagram describing the intermedium process of emitting and absorbing a spin wave by a hole simultaneously has the most significant contribution to the hole self-energy. The hole spectral function retains the features obtained in the one-loop calculation including a quasiparticle peak at the bottom and a few other peaks above it caused by the "string state." The two-loop corrections push these quasiparticle peaks, shifting toward lower energy values, and give a better overall agreement with exact results on the small-size lattice. The spectral functions for a very-large-size lattice are readily obtained numerically; thus this method has a unique advantage in calculating quantities in the thermodynamic limit.

## II. FORMULATION AND NUMERICAL SOLUTIONS

The no-hole ground state is known to be characterized by antiferromagnetic long-range order; thus, the presence of a single hole in an infinite-size lattice does not destroy the long-range order. Therefore, the ground state of the square-lattice Heisenberg antiferromagnet breaks the SU(2) gauge invariance of the Hamiltonian by selecting an axis of staggered magnetization. The loop expansion around this state has been developed where the leading order corresponds to the linear spin-wave approximation.[3] Since the broken gauge invariance of the ground state cannot be restored by the presence of a single hole, it is still a valid starting point to consider fluctuations around the Néel order. The following transformation is the generalization of the definition of spin-deviation operators with respect to the Néel state in the case of the Heisenberg antiferromagnet.[3]

We consider the Néel state as the vacuum state and we define the hole operators which obey Fermi statistics such that $h_i = c_{i\uparrow}^\dagger$ on the $\uparrow$ sublattice and $f_i = c_{i\downarrow}^\dagger$ on the $\downarrow$ sublattice. Hence the other electron operators can be written as

$$\begin{aligned} c_{i\downarrow} &= h_i^\dagger a_i, \quad a_i = S_i^\dagger \quad i \in \uparrow, \\ c_{i\uparrow} &= f_i^\dagger b_i, \quad b_i = S_i^- \quad i \in \downarrow . \end{aligned} \tag{2}$$

The hopping term of the model Hamiltonian (1) now becomes

$$\begin{aligned} \hat{H}_t = -t \sum_{\langle i,j \rangle} \Big[ & (1 - a_i^\dagger a_i) h_i f_j^\dagger b_j \\ & + (1 - b_j^\dagger b_j) f_j h_i^\dagger a_i + \text{H.c.} \Big]. \end{aligned} \tag{3}$$

The Heisenberg term with the presence of a single hole can be written as

$$\hat{H}_s = J \sum_{\langle i,j \rangle} \mathbf{S}_i \cdot \mathbf{S}_j - J \sum_{\langle i,j \rangle} (\hat{n}_i^h \mathbf{S}_i \cdot \mathbf{S}_j + \mathbf{S}_i \cdot \mathbf{S}_j \hat{n}_j^h), \tag{4}$$

where $\hat{n}_i^h = h_i^\dagger h_i$ if $i \in \uparrow$ and $\hat{n}_i^h = f_i^\dagger f_i$ if $i \in \downarrow$. The last term of the above equation gives rise to what we call static vertices that do not contain the hole-hopping parameter $t$ and involve two hole operators and two spin-wave operators in the LSW approximation.

In the previous one-loop (or noncrossing approximation) treatments of the $t$-$J$ model,[7,9] the $\hat{H}_s$ term is treated in a simple way; LSW theory is used to approximate the first term and a Hartree-Fock type of mean-field approximation to treat the static vertices,

$$\begin{aligned} \hat{H}_{\text{HF}} &= \hat{H}_{\text{LSW}} - J \left( \sum_{\langle i,j \rangle} \hat{n}_i^h \langle \mathbf{S}_i \cdot \mathbf{S}_j \rangle + \sum_{\langle i,j \rangle} \langle \mathbf{S}_i \cdot \mathbf{S}_j \rangle \hat{n}_j^h \right) \\ &= \hat{H}_{\text{LSW}} - \sum_i E_h^0 \hat{n}_i^h, \end{aligned} \tag{5}$$

where $\hat{H}_{\text{LSW}}$ is the Heisenberg model in the LSW approximation,

$$\hat{H}_{\text{LSW}} = E_0 \sum_{\mathbf{k}} \Omega_k (\alpha_{\mathbf{k}}^\dagger \alpha_{\mathbf{k}} + \beta_{\mathbf{k}}^\dagger \beta_{\mathbf{k}}), \tag{6}$$

where $E_0$ is the ground-state energy in the linear spin-wave theory and the spin-wave operators $\alpha_{\mathbf{k}}$ and $\beta_{\mathbf{k}}$ are defined as

$$\begin{aligned} \alpha_{\mathbf{k}} &= u_k a_{\mathbf{k}} - v_k b_{-\mathbf{k}}^\dagger, \\ \beta_{\mathbf{k}} &= u_k b_{-\mathbf{k}} - v_k a_{\mathbf{k}}^\dagger, \end{aligned} \tag{7}$$

where the operators $a_{\mathbf{k}}$ and $b_{\mathbf{k}}$ are Fourier transforms of the spin-deviation $a_i$ and $b_i$ operators,

$$\begin{aligned} a_{\mathbf{k}} &= \sqrt{\frac{2}{N}} \sum_{i \epsilon \uparrow} e^{i\mathbf{k}\cdot\mathbf{r}_i} a_i, \\ b_{\mathbf{k}} &= \sqrt{\frac{2}{N}} \sum_{i \epsilon \downarrow} e^{i\mathbf{k}\cdot\mathbf{r}_i} b_i, \end{aligned} \tag{8}$$

and the functions $u_k$ and $v_k$ are given as

$$\begin{aligned} u_k &= \sqrt{\frac{1}{2}\left(\frac{1}{\sqrt{1-\gamma_{\mathbf{k}}^2}} + 1\right)}, \\ v_k &= -\text{sgn}(\gamma_{\mathbf{k}}) \sqrt{\frac{1}{2}\left(\frac{1}{\sqrt{1-\gamma_{\mathbf{k}}^2}} - 1\right)}. \end{aligned} \tag{9}$$

The spin-wave dispersion relation $\Omega_{\mathbf{k}}$ is given in the LSW approximation as $\Omega_{\mathbf{k}} = JzS\sqrt{1-\gamma_{\mathbf{k}}^2}$. The average $\langle\ \rangle$ in Eq. (5) is taken within the LSW approximation and $E_h^0$ is equal to the LSW energy per bond multiplied by 4, namely, $E_h^0 = 2E_0/N$. In the language of diagrammatic perturbation theory, the Hartree-Fock approximation corresponds to the one-loop approximation, as will be shown later.

In the one-loop calculations of the $t$-$J$ model,[4,6–9] the hard-core constraints are neglected; i.e., the factors $(1 - a_i^\dagger a_i)$ and $(1 - b_j^\dagger b_j)$ in the $\hat{H}_t$ are dropped. Thus, the hopping term is approximated by

$$\hat{H}_t' = \sum_{\mathbf{k},\mathbf{q}} g(\mathbf{k},\mathbf{q})\left\{h_{\mathbf{k}}^\dagger f_{\mathbf{k}-\mathbf{q}}\alpha_{\mathbf{q}} + f_{\mathbf{k}}^\dagger h_{\mathbf{k}-\mathbf{q}}\beta_{\mathbf{q}}\right\} + \text{H.c.}, \quad (10)$$

where

$$g(\mathbf{k},\mathbf{q}) = tz\sqrt{\frac{2}{N}}(u_q\gamma_{\mathbf{k}-\mathbf{q}} + v_q\gamma_{\mathbf{k}}). \quad (11)$$

Using a self-consistent perturbation approach where only one-loop diagrams are summed, Dyson's equation for the spinless hole propagator takes the form

$$G(\mathbf{k},\omega) = \frac{1}{\omega - E_h^0 - \sum_{\mathbf{q}} g^2(\mathbf{k},\mathbf{q})G(\mathbf{k}-\mathbf{q},\omega-\Omega_{\mathbf{q}})}. \quad (12)$$

The above equation has been solved numerically on the square lattice by several authors.[7–9]

In this paper, the full $t$-$J$ model is considered. The hopping term contains two types of terms in which one is linear in the spin-deviation operators and another contains three spin-deviation operators. The spin operators in Heisenberg term are expressed in terms of spin-deviation operators ($a_i, a_i^\dagger$ and $b_i, b_i^\dagger$) and then expanded in powers of them in the same way that spin-wave theory is derived.[3] This approach generates an infinite set of terms (vertices). Next, we consider the single-hole Green's function and we imagine all possible one-loop and two-loop diagrammatic contributions to the single-hole self-energy. There is only a finite number of diagrams because only certain vertices can generate up to two-loop diagrams; for example, the diagram with the smallest number of loops which can be generated by a vertex containing two hole and six spin-deviation operators is a three-loop diagram. We develop a self-consistent Dyson's equation that contains all the two-loop diagrams which will be solved numerically on finite but sufficiently large-size lattices.

The entire $H_t$ can be decomposed as $\hat{H}_t = \hat{H}_t' + \hat{H}_t''$ where the remaining terms are given as follows:

$$\hat{H}_t'' = tz\left(\frac{2}{N}\right)^{3/2}\sum_{\mathbf{k},\mathbf{q}_1}\sum_{\mathbf{q}_2,\mathbf{q}_3}\Big\{(u_{\mathbf{q}_1}\alpha_{\mathbf{q}_1}^\dagger + v_{\mathbf{q}_1}\beta_{-\mathbf{q}_1})(u_{\mathbf{q}_2}\alpha_{\mathbf{q}_2} + v_{\mathbf{q}_2}\beta_{-\mathbf{q}_2}^\dagger)(v_{\mathbf{q}_3}\alpha_{-\mathbf{q}_3}^\dagger + u_{\mathbf{q}_3}\beta_{\mathbf{q}_3})h_{\mathbf{k}}f_{\mathbf{k}-\mathbf{q}_1+\mathbf{q}_2+\mathbf{q}_3}^\dagger + (\alpha \longleftrightarrow \beta)(h \longleftrightarrow f)\Big\}\gamma_{\mathbf{k}-\mathbf{q}_1+\mathbf{q}_2} + \text{H.c.} \quad (13)$$

The Hamiltonian $\hat{H}_s$ of Eq. (4) can be rewritten in terms of the operators $a_i$, $b_i$, $h_i$, and $f_i$. We write $\hat{H}_s = \hat{H}_s' + \hat{H}_s'' + \cdots$, where the $\hat{H}_s'$ contains up to quadratic terms in spin-deviation operators, the $\hat{H}_s''$ contains up to quartic terms, etc.,

$$\hat{H}_s' = -\frac{NJ}{2} + 2J\left(\sum_{i\in\uparrow,\delta} a_i^\dagger a_i + \sum_{j\in\downarrow,\delta} b_j^\dagger b_j\right) + \frac{J}{2}\sum_{i\in\uparrow,\delta}(a_i b_{i+\delta} + a_i^\dagger b_{i+\delta}^\dagger) + J - \frac{J}{2}\sum_{i\in\uparrow,\delta} h_i^\dagger h_i(a_i a_i^\dagger + b_{i+\delta}^\dagger b_{i+\delta} + a_i b_{i+\delta} + a_i^\dagger b_{i+\delta}^\dagger) - \frac{J}{2}\sum_{j\in\downarrow,\delta} f_j^\dagger f_j(a_{j+\delta}^\dagger a_{j+\delta} + b_j^\dagger b_j + a_{j+\delta} b_j + a_{j+\delta}^\dagger b_j^\dagger), \quad (14)$$

$$\hat{H}_s'' = -\frac{J}{4}\sum_{i\in\uparrow,\delta}(1 - h_i^\dagger h_i - f_{i+\delta}^\dagger f_{i+\delta})(a_i^\dagger a_i a_i b_{i+\delta} + a_i b_{i+\delta}^\dagger b_{i+\delta} b_{i+\delta} + a_i^\dagger a_i^\dagger a_i b_{i+\delta}^\dagger + a_i^\dagger b_{i+\delta}^\dagger b_{i+\delta}^\dagger b_{i+\delta} + 4a_i^\dagger a_i b_{i+\delta}^\dagger b_{i+\delta}), \quad (15)$$

where $\boldsymbol{\delta}$ is a unit vector connecting nearest neighbors on a square lattice. We can write this Hamiltonian in terms of the Fourier transformation of the hole operators and the spin-wave operators,

$$\hat{H}_s' = \hat{H}_0 + \sum_{\mathbf{k},\mathbf{q},\mathbf{p}}\Big\{h_{\mathbf{k}-\mathbf{p}-\mathbf{q}}^\dagger h_{\mathbf{k}}\tau(\mathbf{q},\mathbf{p})(\beta_{\mathbf{p}}^\dagger\alpha_{\mathbf{q}}^\dagger + \beta_{-\mathbf{p}}\alpha_{-\mathbf{q}}) + h_{\mathbf{k}-\mathbf{p}}^\dagger h_{\mathbf{k}-\mathbf{q}}[\rho_1(\mathbf{q},\mathbf{p})\alpha_{-\mathbf{p}}\alpha_{-\mathbf{q}}^\dagger + \rho_2(\mathbf{q},\mathbf{p})\beta_{-\mathbf{p}}\beta_{-\mathbf{q}}^\dagger] + (h \longleftrightarrow f)(\alpha \longleftrightarrow \beta)\Big\} + \epsilon_0\sum_{\mathbf{k}}(h_{\mathbf{k}}^\dagger h_{\mathbf{k}} + f_{\mathbf{k}}^\dagger f_{\mathbf{k}}), \quad (16)$$

where the unperturbated Hamiltonian $\hat{H}_0$ is

$$\hat{H}_0 = E_0 + J + \sum_{\mathbf{k}} \Omega_{\mathbf{k}} (\alpha^\dagger_{\mathbf{k}} \alpha_{\mathbf{k}} + \beta^\dagger_{\mathbf{k}} \beta_{\mathbf{k}}), \tag{17}$$

where $\Omega_{\mathbf{k}}$ is the energy spectrum of the LSW approximation and the constant $\epsilon_0$ is

$$\epsilon_0 = \frac{2zJ}{N} \sum_{\mathbf{q}} (u^2_{\mathbf{q}} + \gamma_{\mathbf{q}} u_{\mathbf{q}} v_{\mathbf{q}}), \tag{18}$$

and $z$ is the number of neighbors. The functions $\tau(\mathbf{q},\mathbf{p})$, $\rho_1(\mathbf{q},\mathbf{p})$, and $\rho_2(\mathbf{q},\mathbf{p})$ are given by

$$\tau(\mathbf{q},\mathbf{p}) = -\left(\frac{zJ}{N}\right)(\gamma_{\mathbf{q}} v_{\mathbf{q}} v_{\mathbf{p}} + \gamma_{\mathbf{p}} u_{\mathbf{q}} u_{\mathbf{p}} + u_{\mathbf{q}} v_{\mathbf{p}} + \gamma_{\mathbf{q}+\mathbf{p}} v_{\mathbf{q}} u_{\mathbf{p}}), \tag{19}$$

$$\rho_1(\mathbf{q},\mathbf{p}) = -\left(\frac{zJ}{N}\right)(\gamma_{\mathbf{q}} v_{\mathbf{q}} u_{\mathbf{p}} + \gamma_{\mathbf{p}} v_{\mathbf{p}} u_{\mathbf{q}} + u_{\mathbf{q}} u_{\mathbf{p}} + \gamma_{\mathbf{q}-\mathbf{p}} v_{\mathbf{q}} v_{\mathbf{p}}), \tag{20}$$

$$\rho_2(\mathbf{q},\mathbf{p}) = -\left(\frac{zJ}{N}\right)(\gamma_{\mathbf{q}} u_{\mathbf{q}} v_{\mathbf{p}} + \gamma_{\mathbf{p}} u_{\mathbf{p}} v_{\mathbf{q}} + v_{\mathbf{q}} v_{\mathbf{p}} + \gamma_{\mathbf{q}-\mathbf{p}} u_{\mathbf{q}} u_{\mathbf{p}}). \tag{21}$$

We consider the loop expansion of the spinless hole Green's function, namely, the Green's function of the $h^\dagger$ or $f^\dagger$ operator. It is clear that this differs from the physical hole Green's function which is the one probed by photoemission experiments. The real hole Green's function involves the propagator of the true fermion operator that describes the propagation of a spinless hole and spin wave simultaneously and, thus, in this language is not an elementary Green's function. Nevertheless, the spinless hole Green's function, if treated exactly, has poles at those exact eigenstates of the $t$-$J$ Hamiltonian which couple to the no-hole ground state via the spinless hole operator. Figure 1 shows all two-loop diagrams that can be generated by the terms of the expansion of the $t$-$J$ model in spin-deviation operators. Diagrams (a)–(f) are due to $\hat{H}'_t + \hat{H}''_t + \hat{H}'_s$. Diagrams (g) and (h) are due to $\hat{H}''_s$. Note that the two-loop diagram due to the dynamical vertex $\hat{H}'_t$ is zero, as analytically proved in Ref. 9. The contributions to the self-energy $\Sigma(\mathbf{k},\omega)$ from diagrams (a)–(g) are given as follows:

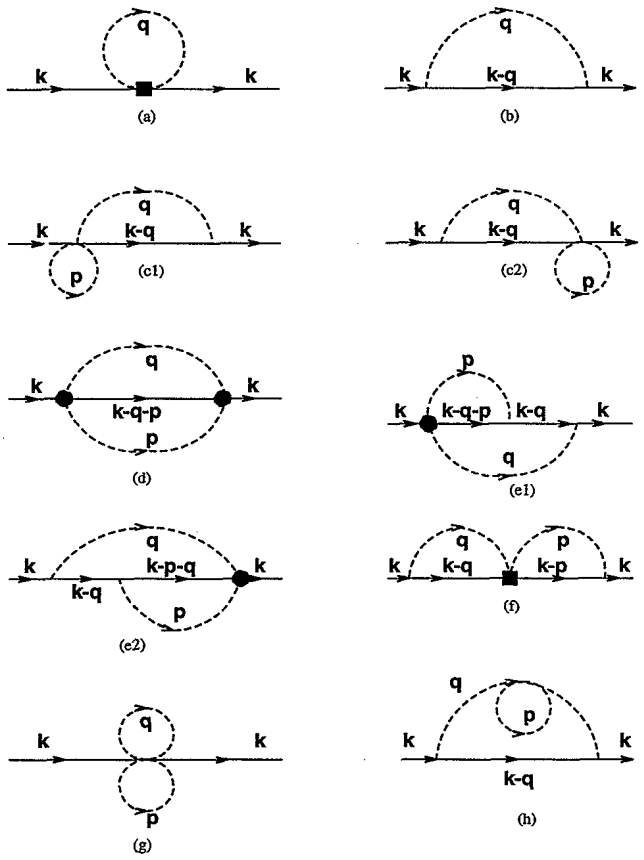


FIG. 1. (a) and (b) are one-loop diagrams and (c)–(h) are two-loop diagrams. Diagrams (e1) and (e2) give the same contribution, and so do diagrams (c1) and (c2).

$$\Sigma_a = -\frac{zJ}{N} \sum_{\mathbf{q}} (2v^2_{\mathbf{q}} + 2u^2_{\mathbf{q}} + 4\gamma_{\mathbf{q}} u_{\mathbf{q}} v_{\mathbf{q}}), \tag{22}$$

$$\Sigma_b(\mathbf{k},\omega) = \sum_{\mathbf{q}} g^2(\mathbf{k},\mathbf{q}) G(\mathbf{k}-\mathbf{q}, \omega - \Omega_{\mathbf{q}}), \tag{23}$$

$$\Sigma_c(\mathbf{k},\omega) = \Sigma_{c_1}(\mathbf{k},\omega) + \Sigma_{c_2}(\mathbf{k},\omega) = \sum_{\mathbf{q}} \zeta\, g^2(\mathbf{k},\mathbf{q}) G(\mathbf{k}-\mathbf{q}, \omega - \Omega_{\mathbf{q}}), \tag{24}$$

$$\Sigma_d(\mathbf{k},\omega) = \sum_{\mathbf{q},\mathbf{p}} \tau^2(\mathbf{q},\mathbf{p}) G(\mathbf{k}-\mathbf{q}-\mathbf{p}, \omega - \Omega_{\mathbf{q}} - \Omega_{\mathbf{p}}), \tag{25}$$

$$\Sigma_e(\mathbf{k},\omega) = \sum_{\mathbf{q},\mathbf{p}} \tau(\mathbf{q},\mathbf{p}) g(\mathbf{k}-\mathbf{q},\mathbf{p}) g(\mathbf{k},\mathbf{q}) G(\mathbf{k}-\mathbf{q}-\mathbf{p}, \omega - \Omega_{\mathbf{q}} - \Omega_{\mathbf{p}}) G(\mathbf{k}-\mathbf{q}, \omega - \Omega_{\mathbf{q}}), \tag{26}$$

$$\Sigma_f(\mathbf{k},\omega) = \sum_{\mathbf{q},\mathbf{p}} \rho_2(\mathbf{q},\mathbf{p}) g(\mathbf{k},\mathbf{q}) g(\mathbf{k},\mathbf{p}) G(\mathbf{k}-\mathbf{q}, \omega - \Omega_{\mathbf{q}}) G(\mathbf{k}-\mathbf{p}, \omega - \Omega_{\mathbf{p}}), \tag{27}$$

$$\Sigma_g = J \left(\frac{z}{N}\right)^2 \left(\sum_{\mathbf{q}} (v^2_{\mathbf{q}} + \gamma_{\mathbf{q}} u_{\mathbf{q}} v_{\mathbf{q}})\right)^2, \tag{28}$$

where $\zeta = \frac{2}{N}\sum_{\mathbf{k}}(1-\sqrt{1-\gamma_{\mathbf{k}}^2})$. Diagram (h) can be thought of as a renormalization of the spin-wave propagator of diagram (b). The contribution of (b) and (h) together correspond to replacing $\Omega_{\mathbf{q}}$ by the renormalized spin-wave spectrum in one loop, $\Omega_{\mathbf{q}}^r = (1+\zeta)\Omega_{\mathbf{q}}$,[3] in the expression for $\Sigma_b$, namely,

$$\Sigma_b'(\mathbf{k},\omega) = \sum_{\mathbf{q}} g^2(\mathbf{k},\mathbf{q}) G(\mathbf{k}-\mathbf{q},\omega-\Omega_{\mathbf{q}}^r). \tag{29}$$

The self-consistent equation for the Green's function including all the diagrams up to two loops is given by the Dyson's equation

$$G(\mathbf{k},\omega) = \frac{1}{\omega-\Sigma_1-\Sigma_2(\mathbf{k},\omega)}, \tag{30}$$

$$\Sigma_2(\mathbf{k},\omega) = \Sigma_b'(\mathbf{k},\omega)+\Sigma_c(\mathbf{k},\omega)+\Sigma_d(\mathbf{k},\omega) +2\Sigma_e(\mathbf{k},\omega)+\Sigma_f(\mathbf{k},\omega). \tag{31}$$

By substituting $u_{\mathbf{q}}$ and $v_{\mathbf{q}}$ into Eqs. (18), (22), and (28) we find that $\Sigma_1 = J+\epsilon_0+\Sigma_a+\Sigma_g = (1+\zeta)^2 J = 2E_0/N$, which is the ground-state energy per bond found in spin-wave theory.[11]

Note that the contributions from diagrams (b), (c1), and (c2) can be combined as

$$\Sigma_b^*(\mathbf{k},\omega) = \Sigma_b(\mathbf{k},\omega) + \Sigma_c(\mathbf{k},\omega) = \sum_{\mathbf{q}} g_r^2(\mathbf{k},\mathbf{q}) G(\mathbf{k}-\mathbf{q},\omega-\Omega_{\mathbf{q}}), \tag{32}$$

where

$$g_r(\mathbf{k},\mathbf{q}) = t^* z\sqrt{\frac{2}{N}}(u_q\gamma_{\mathbf{k}-\mathbf{q}}+v_q\gamma_{\mathbf{k}}). \tag{33}$$

Thus diagrams ($c_1$) and ($c_2$) renormalize the hopping coupling constant from $t$ to $t^*$, which is $t^* = t(1+\zeta)$. This result can also be obtained by a direct Hartree-Fock treatment over the boson operators in the Hamiltonian $\hat{H}_t''$.

It is instructive to study the magnitudes of the contributions of each of the six two-loop diagrams shown in Fig. 1. In order to accomplish this, we replace the hole Green's function $G(\mathbf{k},\omega)$, which is obtained by solving the one-loop self-consistent Dyson's equation (12) on a $4^2$ lattice, into expressions (22)–(28) to calculate these self-energies at $\mathbf{k} = (\frac{\pi}{2},\frac{\pi}{2})$ and $\omega = E(\frac{\pi}{2},\frac{\pi}{2})$, where $E(\frac{\pi}{2},\frac{\pi}{2})$ is the pole of Eq. (12). We chose a $4^2$ lattice to compare the results with available exact results.

As can be noticed in Table I, the contribution from $\Sigma_d$ is very small. This is expected because diagram (d) shown in Fig. 1 contains only static vertices; thus it gives a correction to the mean-field Hartree-Fock result. We know that the static single-hole energy $E_h^0$ obtained from the mean-field calculation is very close to the exact result.[13,14] Thus the correction to $E_h^0$ was expected to be small. The contributions from diagrams (e1) and (e2) are identical. Notice, however, that the contribution of $\Sigma_f$ is much larger than that of $\Sigma_e$ even though diagrams (e) and (f) in Fig. 1 have similar structure. Diagrams (c1) and (c2) renormalize the hopping parameter from $t$ to $t^*$, which is $1.158t$ in the thermodynamic limit and gives rise to a significant change to the one-loop results. The physics process can be viewed as an enhancement of the hole mobility due to spin-wave fluctuations. As a summary, we identify that the two-loop diagrams (c) and (f) are the most significant ones that give the major corrections to the one-loop results.

Dyson's equation (30) that includes all the two-loop diagrams can be solved self-consistently on finite- but large-size lattices. The single-hole energies obtained from such self-consistent solution on a $4^2$ lattice are shown in Fig. 2, where all the energies correspond to the momentum state $\mathbf{k} = (\frac{\pi}{2},\frac{\pi}{2})$. For the sake of comparison, we include one-loop solutions (vertical crosses), two-loop self-consistent solutions (diamonds), and exact diagonalization results (squares). We can see that considerable improvement is obtained by including two-loop diagrams.

The inclusion of two-loop diagrams also improves markedly the single-hole energies at other momenta. In Table II, we show the hole band calculated for different $J/t$ on a $4^2$ lattice. The numbers in the table are obtained by solving the two-loop self-consistent Dyson's equation (30) while the numbers in parentheses are exact diagonalization results. The results of the one-loop calculations are also included in the table for comparison.

TABLE I. The real part of the self-energies calculated on a $4\times4$ lattice at $\mathbf{k} = (\frac{\pi}{2},\frac{\pi}{2})$ and $\omega = E(\frac{\pi}{2},\frac{\pi}{2})$.

| $J/t$ | $\Sigma_b^*$ | $\Sigma_d$ | $\Sigma_e$ | $\Sigma_f$ |
|---|---|---|---|---|
| 0.10 | -2.600 | -0.001 | -0.011 | -0.128 |
| 0.20 | -2.157 | -0.003 | -0.017 | -0.186 |
| 0.30 | -1.989 | -0.005 | -0.021 | -0.186 |
| 0.40 | -1.707 | -0.007 | -0.025 | -0.218 |
| 0.55 | -1.328 | -0.011 | -0.028 | -0.252 |
| 0.70 | -0.959 | -0.016 | -0.030 | -0.269 |
| 0.83 | -0.668 | -0.020 | -0.030 | -0.277 |

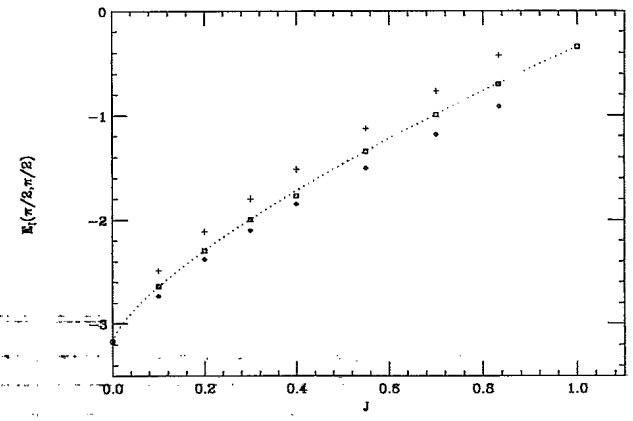


FIG. 2. The hole energies at momentum $\mathbf{k} = (\frac{\pi}{2},\frac{\pi}{2})$ calculated on a $4^2$ lattice as a function of $J/t$. The vertical crosses are one-loop solutions, the diamonds are self-consistent two-loop solutions, and the squares are exact results taken from Refs. 11 and 12.

TABLE II. The hole energies calculated self-consistently by including all two-loop diagrams on a $4^2$ lattice for different momenta are compared to those obtained by a one-loop calculation (given in square brackets) and by exact diagonalization (given in parentheses).

| k | $J/t = 0.2$ | $J/t = 0.4$ | $J/t = 0.7$ |
|---|---|---|---|
| (0,0) | -1.921[-1.682](-2.028) | -1.037[-0.766](-1.055) | -0.019[0.255](0.045) |
| $(\frac{\pi}{2}, 0)$ | -2.222[-1.964](-2.149) | -1.620[-1.300](-1.461) | -0.922[-0.526](-0.648) |
| $(\frac{\pi}{2}, \frac{\pi}{2})$ | -2.380[-2.120](-2.298) | -1.850[-1.522](-1.722) | -1.184[-0.774](-0.993) |

The spectral function $A(\mathbf{k} = (\frac{\pi}{2}, \frac{\pi}{2}), \omega)$ obtained by solving the two-loop Dyson's equation (30) on a $4^2$ lattice (solid line) is compared with the exact results (dotted line) in Fig. 3. By comparing with the results shown in Ref. 9, we find that the general shapes of the spectral functions are not changed by the inclusion of two-loop diagrams in the calculation, except that the quasiparticle peaks shift toward the lower-energy values and closer to the exact results. This is true for the spectral functions corresponding to other momentum states as well. Thus the hole bandwidth and spectral weight do not have significant changes due to the two-loop diagrams. More importantly, the peaks corresponding to the "string" states above the lowest-energy peaks appearing in the spectral function of one-loop calculations are also well defined by including the two-loop contribution. In Fig. 4, we show the spectral function for $\mathbf{k} = (\frac{\pi}{2}, \frac{\pi}{2})$ obtained on a $20^2$ lattice, which is a solution of the self-consistent calculation including the dominant two-loop diagrams. As we see, the "string" states remain robust.

In Table III, we report a self-consistent two-loop calculation on a $20^2$ lattice. The calculation only includes the dominant two-loop diagrams, shown in Figs. 1(c) and 1(f), because in this case the calculation can be factorized into a product of two one-loop diagrams; thus the CPU time required in the calculation is not too demanding. If we compare with one-loop calculations, we can see that the changes of spectral weights and hole bandwidth are indeed small compared to the changes to the hole ground-state energies. In Fig. 5, we show the hole energy dispersion $E(\mathbf{k})$ along the path $\Gamma M X \Gamma$ shown as an inset as calculated on a $20^2$ size lattice and for $J/t = 0.2$. This curve can be compared with Fig. 13 of Ref. 9. Notice that the effect of two-loop diagrams is to shift the spectrum to more negative values of the energy but it does not significantly affect its overall shape, i.e., its bandwidth, the minimum at $(\pi/2, \pi/2)$, etc. In Fig. 6 we show the calculated $Z(\mathbf{k})$ along the same path, on the same size lattice, and with the same value of $J/t$. We find that the quasihole is best defined at $\mathbf{k} = (\pi/2, \pi/2)$ and at $\mathbf{k} = (\pi, 0)$.

It is interesting to note that the renormalization factor $\zeta$ to the hopping energy $t$ is identical to that of the higher-order 1/S correction to the LSW energy spectrum of the spin-1/2 Heisenberg model on a square lattice. Recall that the spin-wave velocity is renormalized by a factor of 1.158. This does not come as a total surprise, because in the context of loop expansion the spin-wave theory of the Heisenberg model[11,3] is indeed a one-loop-higher correction to the LSW theory. Analogous to the case of the Heisenberg model, our two-loop correction to the single-hole energy is "overcorrected" in the sense that the dif-

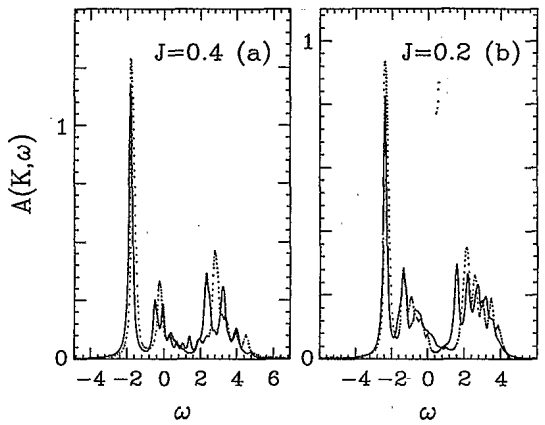


FIG. 3. The hole spectral function $A(\mathbf{k} = (\frac{\pi}{2}, \frac{\pi}{2}), \omega)$ calculated on a $4^2$ lattice for $J/t = 0.2$ and 0.4, respectively. The solid line denotes two-loop self-consistent solution, while the dotted line refers to the exact result taken from Ref. 11.

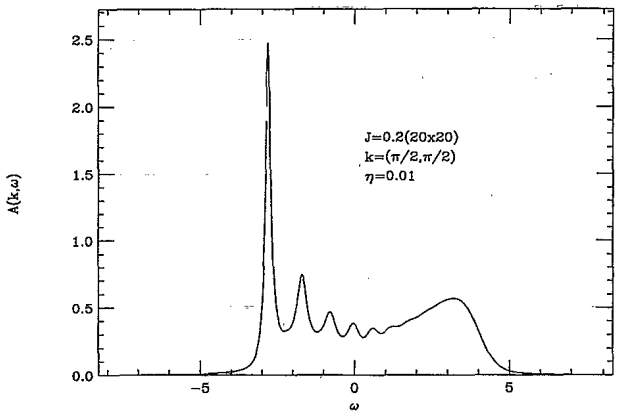


FIG. 4. The hole spectral function $A(\mathbf{k} = (\frac{\pi}{2}, \frac{\pi}{2}), \omega)$ calculated self-consistently including the dominant two-loop diagrams on a $20^2$ lattice for $J = 0.2$.

TABLE III. The energy, residue, and bandwidth of the quasiparticle peak at $\mathbf{k} = (\frac{\pi}{2}, \frac{\pi}{2})$ calculated self-consistently up to two-loop level on a $20^2$ lattice. The corresponding one-loop results are given in parentheses for comparison. The values of $\eta = 0.01$ and $\Delta\omega = 0.006$ have been used.

| $J/t$ | $E(\frac{\pi}{2}, \frac{\pi}{2})$ | $Z(\frac{\pi}{2}, \frac{\pi}{2})$ | $W$ |
|---|---|---|---|
| 0.10 | -3.168(-2.519) | 0.121(0.138) | 0.235(0.237) |
| 0.20 | -2.816(-2.279) | 0.207(0.222) | 0.443(0.424) |
| 0.30 | -2.511(-1.967) | 0.272(0.287) | 0.616(0.600) |
| 0.40 | -2.241(-1.685) | 0.328(0.342) | 0.782(0.748) |
| 0.55 | -1.868(-1.297) | 0.399(0.411) | 0.989(0.888) |
| 0.70 | -1.515(-0.938) | 0.456(0.464) | 1.121(0.955) |

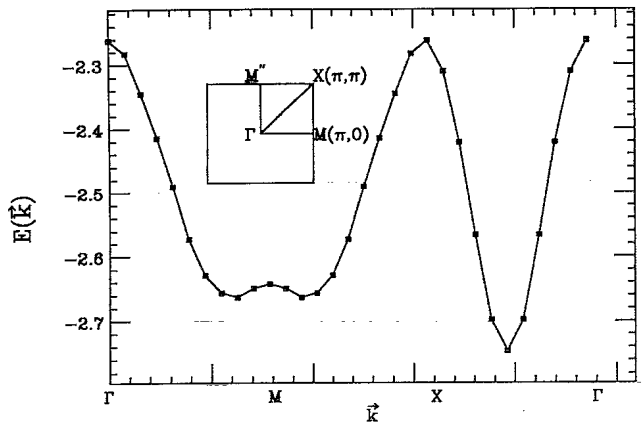


FIG. 5. The hole energy $E(\mathbf{k})$ calculated self-consistently including the dominant two-loop diagrams on a $20^2$ lattice for $J = 0.2$.

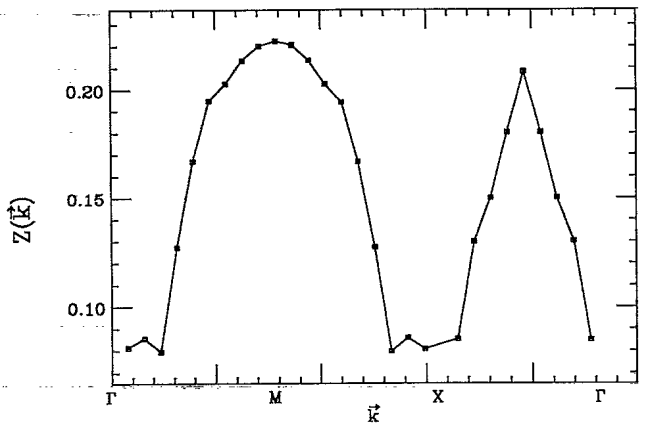


FIG. 6. The hole spectral weight $Z(\mathbf{k})$ calculated self-consistently including the dominant two-loop diagrams on a $20^2$ lattice for $J = 0.2$.

ference between the loop expansion results and the exact values changes sign as we go from one-loop to two-loop expansion although the absolute value of this difference is markedly smaller, as illustrated in Fig. 2.

## III. CONCLUSION

The satisfactory agreement of our two-loop expansion calculation with the exact results on a small lattice results largely from the fact that our hopping Hamiltonian (13) takes into account the hard-core constraints that are neglected in the one-loop calculation. We argue that the effect of the two-loop diagrams is analogous to the higher-order nonlinear spin-wave correction to the LSW theory of the Heisenberg model. Our loop expansion may also be regarded as an expansion of $1/z$ as in the case of the diagrammatic calculation of the spin-wave theory of the Heisenberg model, although we could not provide a rigorous proof here. In addition, the vertex that describes the simultaneous emission and absorption of a spin wave by a hole is identified as a more important contributor than others to the single-hole energy. We believe that the method provides a reliable tool to carry out further calculations of the $t$-$J$ model in the physical region of $J/t < 1$. Interesting problems such as hole-pairing symmetry and the interaction between two holes are possible to be studied using the two-loop diagrammatic expansion which is one of the few available analytic approaches.

## ACKNOWLEDGMENTS

One of us (Z.L.) would like to thank Professor Geoffrey Chester and Professor Malvin Kalos for reading the manuscript and for their encouragement. This work was supported in part by the National Science Foundation (NSF) under Grant No. DMR-9200469 and by the Office of Naval Research under Grant No. N00014-93-1-0189.

[1] W. F. Brinkman and T. M. Rice, Phys. Rev. B **2**, 1324 (1970).
[2] J. G. Bednorz and K. A. Müller, Z. Phys. B **64**, 188 (1986).
[3] E. Manousakis, Rev. Mod. Phys. **63**, 1 (1991).
[4] C. Kane, P. Lee, and N. Read, Phys. Rev. B **39**, 6880 (1989).
[5] R. B. Laughlin, Phys Rev. B **45**, 400 (1992).
[6] S. Schmitt-Rink, C. M. Varma, and A. E. Ruckenstein, Phys. Rev. Lett. **60**, 2793 (1988).
[7] G. Martínez and P. Horsch, Phys. Rev. B **44**, 317 (1991).
[8] F. Marsiglio, A. Ruckenstein, S. Schmitt-Rink, and C. Varma, Phys. Rev. B **43**, 10 882 (1991).
[9] Z. Liu and E. Manousakis, Phys. Rev. B **44**, 2414 (1991); **45**, 2425 (1991).
[10] P. W. Anderson, Phys. Rev. **86**, 694 (1952).
[11] R. Kubo, Phys. Rev. **87**, 568 (1952); T. Oguchi, *ibid.* **117**, 117 (1960).
[12] E. Dagotto, R. Joynt, A. Moreo, S. Bacci, and E. Gagliano, Phys. Rev. B **41**, 9049 (1990).
[13] T. Barnes, A. E. Jacobs, M. D. Kovarik, and W. G. Macready, Phys. Rev. B **45**, 256 (1992).
[14] N. Bulut, D. Hone, D. J. Scalapino, and E. Y. Loh, Phys. Rev. Lett. **62**, 2192 (1989).